

## Molecular Crystals and Liquid Crystals Science and Technology. Section A. Molecular Crystals and Liquid Crystals

Publication details, including instructions for authors and  
subscription information:

<http://www.tandfonline.com/loi/gmcl19>

### A Calorimetric Study of Phase Separation in Liquid Crystal/Matrix Systems: Determination of the Excess Specific Heat of Mixing

George W. Smith<sup>a</sup>

<sup>a</sup> Physics Department, General Motors Research, Warren,  
Michigan, 48090-9055

Version of record first published: 04 Oct 2006.

To cite this article: George W. Smith (1994): A Calorimetric Study of Phase Separation in Liquid Crystal/Matrix Systems: Determination of the Excess Specific Heat of Mixing, *Molecular Crystals and Liquid Crystals Science and Technology. Section A. Molecular Crystals and Liquid Crystals*, 239:1, 63-85

To link to this article: <http://dx.doi.org/10.1080/10587259408047172>

PLEASE SCROLL DOWN FOR ARTICLE

Full terms and conditions of use: <http://www.tandfonline.com/page/terms-and-conditions>

This article may be used for research, teaching, and private study purposes. Any substantial or systematic reproduction, redistribution, reselling, loan, sub-licensing, systematic supply, or distribution in any form to anyone is expressly forbidden.

The publisher does not give any warranty express or implied or make any representation that the contents will be complete or accurate or up to date. The accuracy of any instructions, formulae, and drug doses should be independently verified with primary sources. The publisher shall not be liable for any loss, actions, claims, proceedings, demand, or costs or damages whatsoever or howsoever caused arising directly or indirectly in connection with or arising out of the use of this material.

# A Calorimetric Study of Phase Separation in Liquid Crystal/Matrix Systems: Determination of the Excess Specific Heat of Mixing

GEORGE W. SMITH

*Physics Department, General Motors Research, Warren, Michigan 48090-9055*

*(Received April 30, 1993; in final form May 6, 1993)*

The effects of concentration and state of cure on mixing and phase separation of binary systems of a low molecular weight liquid crystal (LC) and an organic matrix have been determined for the first time. We found that, as temperature is increased, mixing in uncured LC/matrix systems is accompanied by a step-like decrease in specific heat at  $T_{\text{mix}}$ , the mixing temperature. This decrease is due, for the most part, to the (negative) excess specific heat of mixing,  $\Delta C_{\text{mix}}$ . The excess enthalpy of mixing,  $\Delta H_{\text{mix}}$ , may also contribute to the thermal effect. A plot of  $\Delta C_{\text{mix}}$  versus LC concentration exhibits a minimum, as expected from theory. Such a plot for a mixture of a specific LC (E7) with uncured matrix (NOA65) allows us to estimate the solubility limit of E7 in the matrix-rich phase (~15%) and of NOA65 in the LC-rich phase (~5%).

Uncured E7/NOA65 mixtures exhibit phase diagrams with an upper critical solution temperature (UCST) slightly above 300 K. To avoid undesired phase separation prior to final cure, the formation temperature for an E7/NOA65 polymer-dispersed liquid crystal (PDLC) should thus be suitably higher than 300 K. The phase diagram of uncured LC/matrix mixtures can be computed using Flory-Huggins theory. The F-H model also predicts the correct sign for  $\Delta C_{\text{mix}}$ , but is less successful in calculating its magnitude.

The extent (or degree) of matrix cure plays the major role in phase separation of LC/matrix mixtures to form a PDLC. Partially-cured samples exhibit mixing transitions which do not disappear until the final stages of the cure process. Only during the last 10%, or so, of cure does phase separation of the LC from the matrix become fixed. Once this has occurred, a fraction of the LC is permanently phase-separated, with the rest dissolved in the matrix. The appearance of a nematic-isotropic (NI) transition during the final cure stages confirms that phase separation has become more or less "frozen in"; the magnitude of the NI transition enthalpy makes it possible to estimate the amount of LC dissolved in the matrix. The temperature of the NI transition for incomplete cure is nearly coincident with  $T_{\text{mix}}$ , perhaps due to greater solubility of the polymer in the isotropic phase than in the nematic.

**Keywords:** *phase separation, mixing, binary systems, liquid crystals, polymers, solubility*

## INTRODUCTION

Understanding of phase separation in binary systems of a low molecular weight liquid crystal (LC) and an organic matrix is becoming increasingly important, partially due to efforts to improve materials and fabrication methods for polymer-

dispersed liquid crystal (PDLC) films.<sup>1-4</sup> These films, dispersions of micron-sized droplets of liquid crystal in a polymer matrix, have considerable potential for several applications, including variable transparency windows and displays. PDLCs are formed by a two-step process: 1) a liquid crystal and a polymer precursor are initially mixed together to form a uniform solution; 2) the polymer matrix is hardened, during which process LC phase-separates from the polymer in the form of microdroplets. The hardening can be carried out by several techniques<sup>1-4</sup>: 1) polymerization of the precursor to produce either a linear (thermoplastic) or a cross-linked (thermoset) matrix; 2) cooling of a thermoplastic polymer/LC mixture; or 3) evaporation of a common solvent in which both LC and thermoplastic are dissolved. The polymerization process of method 1) can be induced either by a thermal cure<sup>1,3,5,6</sup> or by curing using ultraviolet (UV)<sup>2,7,8</sup> or electron-beam<sup>9</sup> irradiation. Our research efforts have focussed primarily on UV-curing techniques to produce PDLCs based on a highly cross-linked matrix.<sup>2,7,8</sup>

Two aspects of phase separation are especially important to understanding the formation of a UV-cured PDLC. The first of these concerns the solubility behavior of the uncured LC/matrix mixture, a system characterized by a phase diagram with an upper critical solution temperature (UCST).<sup>10,11</sup> Before cure, the temperature,  $T$ , of the mixture should be higher than  $T_{\text{mix}}$ , the mixing temperature (above which the UCST components are co-dissolved). If  $T$  is below this value, undesirable phase separation prior to cure may lead to the formation of large droplets or "puddles" of liquid crystal, resulting in non-uniform optical properties of the PDLC film. (As we shall see,  $T_{\text{mix}}$  increases during cure, suggesting that the formation temperature should therefore be suitably higher than the mixing temperature of the system during cure.) The second aspect is the "demixing" of the liquid crystal from the matrix which occurs as the curing reactions proceed, a process which may involve either nucleation and growth or spinodal decomposition.<sup>11</sup>

In the present paper we consider mixing and phase separation both in the uncured state and at intervals during the cure process. We report the first direct measurements of the excess specific heat of mixing,  $\Delta C_{\text{mix}}$ , of liquid crystal/polymer mixtures under both sets of circumstances: 1) By means of differential scanning calorimetry (DSC), we have examined the phase behavior of uncured LC/matrix mixtures as a function of LC content. DSC thermal spectra reveal an apparent decrease in specific heat ( $\Delta C_{\text{mix}} < 0$ ) as the temperature is increased through the mixing temperature,  $T_{\text{mix}}$ . (As we shall see, such a decrease is consistent with UCST phase behavior.) In order to confirm that the observed decrease is due, at least in part, to  $\Delta C_{\text{mix}}$ , we also used DSC to measure the specific heats of the mixtures and of their components. 2) In addition, by means of DSC we investigated the effect of degree of matrix cure,  $D_{\text{cure}}$ , on phase behavior and phase separation of two LCs in a UV-curable matrix. Phase separation was never complete, even in a fully cured PDLC; measurement of the fraction of LC remaining dissolved in the polymer matrix has been discussed in several publications,<sup>5,6,12</sup> and solubility models have also been developed.<sup>5,6,11,12</sup> We shall extend those studies by examining  $\Delta C_{\text{mix}}$  in terms of the Flory-Huggins<sup>13-16</sup> model for phase separation in binary systems. Before we describe our work, let us review previous studies on polymer/polymer, gel, and LC/polymer systems.

## BACKGROUND: PRIOR STUDIES

### Polymer/Polymer Systems

In 1984 ten Brinke and Karasz<sup>17</sup> developed a theory for binary polymer blends which allowed them to calculate  $\Delta C_{\text{mix}}$  for a mixture exhibiting a LCST (lower critical solution temperature) phase diagram (i.e., the system demixes above  $T_{\text{mix}}$ ). They predicted that  $\Delta C_{\text{mix}}$  for a LCST system should be positive and on the order of  $10^{-2}$  cal/g-K, pointing out that this magnitude is well within the scope of experimental measurement techniques. Subsequently, Barnum *et al.*<sup>18</sup> used DSC to measure  $\Delta C_{\text{mix}}$ , obtaining a maximum value of +0.02 cal/g-K for a miscible LCST blend. They did not determine  $\Delta C_{\text{mix}}$  by scanning the DSC sample temperature through the mixing range. Rather, they measured the specific heats of the binary mixture and of the two components and determined the excess quantity from:

$$\Delta C_{\text{mix}} = C_b - [zC_1 + (1 - z)C_2] \quad (1a)$$

$$= C_b - [x\rho_1 C_1 + (1 - x)\rho_2 C_2]/[\rho_2 - (\rho_2 - \rho_1)x], \quad (1b)$$

where  $C_b$ ,  $C_1$ , and  $C_2$  are specific heats of the binary mixture and components 1 and 2,  $z$  and  $x$  are the mass and volume fractions of component 1, and  $\rho_1$  and  $\rho_2$  are the corresponding densities. It is clear that, for  $\rho_1 = \rho_2$ ,  $x \equiv z$ .

Four groups of workers<sup>19–22</sup> have used DSC to investigate the enthalpy of mixing,  $\Delta H_{\text{mix}}$ , of polymer blends with LCST phase diagrams. (It is impossible to measure  $\Delta H_{\text{mix}}$  directly by mixing the blend components together.<sup>20,23</sup>) The groups operated the calorimeter in the heating mode so that the heat of demixing (phase separation) was actually detected rather than  $\Delta H_{\text{mix}}$  itself. Natansohn<sup>19</sup> pointed out that  $\Delta H_{\text{mix}}$  should be negative (exothermic). Both Ebert *et al.*<sup>20</sup> and Uriarte *et al.*<sup>21</sup> observed endothermic peaks (about 0.2 to 0.5 cal/g) associated with phase separation, showing that, as expected,  $\Delta H_{\text{mix}}$  is negative for their LCST systems. Moore and Kim<sup>22</sup> also found an endothermic peak due to demixing; since their system redissolved rapidly when  $T$  was decreased, they were also able to observe an exothermic mixing peak upon cooling. On the other hand, when Natansohn<sup>19</sup> heated his LCST system through the demixing temperature, he found an exothermic peak, a seemingly surprising observation since it implies  $\Delta H_{\text{mix}} > 0$ . However, Natansohn did not discuss this point in any detail.

Using the technique of Barnum *et al.*, the Uriarte group also attempted to measure the excess specific heat for their blend. They determined  $\Delta C_{\text{mix}}$  to be  $\sim 0.004$  cal/g-K, about equal to their experimental uncertainty and an order of magnitude smaller than the Barnum result for a different blend. The Uriarte group also calculated the enthalpy of mixing as a function of temperature. The computed value of  $\Delta H_{\text{mix}}$  increased from about  $-0.6$  to  $-0.2$  cal/g as  $T$  increased from 313 K to 433 K. From  $\Delta H_{\text{mix}}$  they calculated  $\Delta C_{\text{mix}}$  using

$$\Delta C_{\text{mix}} = (\delta \Delta H_{\text{mix}} / \delta T)_p. \quad (2)$$

They computed  $\Delta C_{\text{mix}}$  to be 0.003 cal/g-K at 390 K, in agreement with their ex-

periment. However, they also pointed out that, although the resulting  $\Delta C_{\text{mix}}$  was positive (in accord with the result of ten Brinke and Karasz<sup>17</sup>), its magnitude increased with temperature (opposite behavior to that of Reference 17).

### Cyclohexanol/Polystyrene Gel

Hikmet *et al.*<sup>24</sup> have investigated the phase behavior of a cyclohexanol/polystyrene gel, a UCST system. They determined the phase diagram of the gel from light scattering studies and used DSC to measure the glass transition temperature,  $T_g$ . They noted, without further comment, that, in addition to the glass transition, the DSC thermal spectra showed a "second, higher temperature step" at the temperature where turbidity disappeared (i.e., at  $T_{\text{mix}}$ ). Its sense was opposite to that of the step at  $T_g$ : i.e., whereas the specific heat *increased* at the glass transition by an amount  $\Delta C_g$ , the higher temperature step corresponded to a *decrease*. We estimate the magnitude of the decrease to be  $\sim 0.5 \Delta C_g$ . We believe that this second step was due, at least in part, to the excess specific heat of mixing,  $\Delta C_{\text{mix}}$  (see below).

### LC/Polymer Blends

Ahn *et al.*<sup>25</sup> have used DSC and optical microscopy to examine phase behavior of blends of a low molecular weight LC and two amorphous polymers. They also reviewed the previous literature and concluded that the heat flow involved in the phase separation process is too small for detection using DSC. As we shall see below, DSC can indeed be used to measure the excess specific heat of mixing of a LC/polymer mixture. Let us now examine the implications of Flory-Huggins theory relative to  $\Delta H_{\text{mix}}$  and  $\Delta C_{\text{mix}}$ .

### FLORY-HUGGINS THEORY: $\Delta H_{\text{mix}}$ AND $\Delta C_{\text{mix}}$

The phase stability of a mixture of two components can be understood in terms of the lattice theory of Flory and Huggins.<sup>13</sup> The starting point of the model is the Gibbs free energy of mixing,  $\Delta G_{\text{mix}}$ , given by:

$$\Delta G_{\text{mix}} = \Delta H_{\text{mix}} - T\Delta S_{\text{mix}}, \quad (3)$$

where  $\Delta H_{\text{mix}}$  is the enthalpy of mixing,  $\Delta S_{\text{mix}}$  the entropy of mixing, and  $T$  the absolute temperature. For mixing of the two components to occur,  $\Delta G_{\text{mix}}$  should be less than 0. According to the F-H theory,  $\Delta S_{\text{mix}}$  is

$$\Delta S_{\text{mix}} = -NR[(1 - \phi)\ln(1 - \phi)/m_1 + \phi \ln \phi/m_2]. \quad (4)$$

Here  $m_1$  and  $m_2$  are the degree of polymerization of components 1 (LC in our case) and 2 (matrix),  $\phi$  is the volume fraction of component 2,  $R$  is the gas constant, and  $N$  is the number of moles of polymer segments in the system. It is apparent from Equation 4 that as  $m_1$  and  $m_2$  increase,  $\Delta S_{\text{mix}}$  approaches 0, making it difficult

for high polymers to mix unless  $\Delta H_{\text{mix}}$  becomes small or negative. Indeed, 95% of all binary polymer blends are incompatible.<sup>15</sup>

The F-H enthalpy of mixing can be expressed as

$$\Delta H_{\text{mix}} = NRT\chi\phi(1 - \phi) \quad (5)$$

where  $\chi$  is the well-known Flory-Huggins interaction parameter. The temperature dependence of  $\chi$  is often given by<sup>14,26,27</sup>

$$\chi(T) = C + D/T, \quad (6)$$

where  $C$  and  $D$  are frequently taken to be constants. Equation 6 introduces the temperature into phase diagrams derived from the F-H theory. For some systems  $\chi$  may be a function of  $\phi$  as well.<sup>26</sup> However, we shall not be concerned with either  $\phi$ -dependence of  $\chi$  or polydispersity of  $m_1$  and  $m_2$ .

Nishi<sup>14</sup> showed that the proper choice of the signs of  $C$  and  $D$  leads to the two major types of binary phase diagrams: i) For  $C < 0$  and  $D > 0$ , the polymers phase-separate upon cooling below  $T_{\text{mix}}$  (UCST behavior). The maximum value of  $T_{\text{mix}}$  is the critical temperature,  $T_c$ , which is attained at a critical composition,  $\phi_c$ . ii) For  $C > 0$  and  $D < 0$ , phase separation occurs upon heating above  $T_{\text{mix}}$  (LCST behavior), and  $T_c$  is the minimum value of  $T_{\text{mix}}$ . Unfortunately, Nishi incorrectly stated that the compatibility regions for the two systems lie *below* the line  $C = -D/T$ . Careful examination of inequality relations derived for the two types of phase behavior shows that both regions actually lie *above* the line. This point is discussed in the Appendix.

UCST phase diagrams are less common than LCST among binary polymer systems.<sup>15</sup> However, systems such as PDLCS, in which the liquid crystal (component 1) has a low molecular weight, readily exhibit UCST behavior. The F-H theory has had a certain degree of success in describing phase behavior of both polymer blends<sup>14,15,27</sup> and PDLCS.<sup>10,11</sup>

### Enthalpy of Mixing

The critical temperature from the F-H theory is given by<sup>14</sup>:

$$T_c = (-D/C)\{1 - (1/2C)[m_1^{-0.5} + m_2^{-0.5}]^2\}^{-1}, \quad (7)$$

and the critical composition by:

$$\phi_c = [1 + (m_2/m_1)^{0.5}]^{-1}. \quad (8)$$

By substituting Equations 6–8 into Equation 5 we obtain the following expression for  $\Delta H_{\text{mix}}$  at the critical temperature:

$$\Delta H_{\text{mix}}^c/NR = D/\{(m_1 m_2)^{0.5}[-C + 0.5\{m_1^{-0.5} + m_2^{-0.5}\}^2]\}. \quad (9)$$

As we shall see, this expression is always positive for physically meaningful values of the parameters.

### UCST System

We can determine the expected sign of  $\Delta H_{\text{mix}}$  by using inequality relations derived in the Appendix. From Equations 5 and 6 we have

$$\Delta H_{\text{mix}} = NR\phi(1 - \phi)(CT + D). \quad (10)$$

From inequality A5,

$$C = -D/T + \epsilon, \quad (11)$$

where  $\epsilon$  is positive definite. Thus, Equation 10 becomes

$$\Delta H_{\text{mix}} = NRT\phi(1 - \phi)\epsilon, \quad (12)$$

where all terms on the right hand side of the equation are positive. Thus, Flory-Huggins predicts a positive enthalpy of mixing for a UCST binary. The magnitude of the critical value can be determined from Equation 9 for appropriate values of  $C$ ,  $D$ ,  $m_1$ , and  $m_2$ . As we shall see below, the phase diagram of our uncured LC/matrix mixture is described fairly well by choosing  $C = -0.2$ ,  $D = 230 \text{ K}$ ,  $m_1 = 2$ , and  $m_2 = 8$ . Substitution of these parameters into Equation 9 yields  $\Delta H_{\text{mix}}^c = 75 \text{ cal/mole}$  (or, for a monomer molecular weight of about 100,  $\sim 0.7 \text{ cal/g}$ ). If  $m_1$  is fixed at 2, the value of  $\Delta H_{\text{mix}}^c$  calculated from Equation 9 decreases from  $\sim 95 \text{ cal/mole}$  to  $\sim 11 \text{ cal/mole}$  as  $m_2$  increases from 2 to 1000.

### LCST System

Inequality A11 of the Appendix shows that Equations 11 and 12 apply to LCST as well as to UCST systems. Thus, the simple F-H model predicts  $\Delta H_{\text{mix}} > 0$  for both LCST and UCST binary mixtures. This prediction is in accord with the fact that Equation 9 yields positive values of  $\Delta H_{\text{mix}}^c$  using typical LCST parameters of Nishi<sup>14</sup> ( $C = 0.5$ ,  $D = -186.5 \text{ K}$ ,  $m_1 = 100$ ):  $\Delta H_{\text{mix}}^c$  decreases from  $\sim 14 \text{ cal/mole}$  to  $\sim 1.2 \text{ cal/mole}$  as  $m_2$  increases from 10 to 1000.

However, since it predicts  $\Delta H_{\text{mix}} > 0$  for both UCST and LCST, the F-H model is in disagreement with several experiments<sup>20-22</sup> and with the model calculation of Uriarte *et al.*<sup>21</sup> On the other hand, Natansohn's results<sup>19</sup> seem to suggest  $\Delta H_{\text{mix}} > 0$  for at least one LCST system. Let us now turn our attention to Flory-Huggins predictions for  $\Delta C_{\text{mix}}$ .

### Excess Specific Heat of Mixing

Equations 2, 5, and 6 give the simple result that

$$\begin{aligned} \Delta C_{\text{mix}}/NR &= C\phi(1 - \phi) \\ &= Cx(1 - x), \end{aligned} \quad (13)$$

where  $x (= 1 - \phi)$  is the LC volume fraction.<sup>28</sup> Equation 13 leads to the obvious conclusions that  $\Delta C_{\text{mix}} < 0$  for UCST systems and  $\Delta C_{\text{mix}} > 0$  for LCST systems. The predicted sign for the LCST case is in accord with the results of the models of References 17 and 21. However, the magnitudes of  $\Delta C_{\text{mix}}$  from Equation 13 for a monomer molecular weight of  $\sim 100$  and typical  $C$ -values (ranging from  $\sim -0.5$  for UCST systems to  $\sim +0.5$  for LCST) are roughly  $10^{-3}$  cal/g-K, about 10 times smaller than given by the model of ten Brinke and Karasz<sup>17</sup> and by the Barnum<sup>18</sup> experiment, but in agreement with the experiment and theory of Uriarte *et al.*<sup>21</sup> Although the paper of ten Brinke and Karasz<sup>17</sup> dealt only with the LCST case, Karasz<sup>29</sup> has pointed out that their model would predict  $\Delta C_{\text{mix}} < 0$  for a UCST system. Thus, both the F-H and ten Brinke/Karasz models are in apparent agreement as to the sign of  $\Delta C_{\text{mix}}$  for both LCST and UCST mixtures. However, as we have seen, F-H fails in other details concerning  $\Delta C_{\text{mix}}$  and  $\Delta H_{\text{mix}}$ .

## EXPERIMENTAL ASPECTS

### Materials and Sample Preparation

**Liquid Crystals.** Two LCs were employed in these studies: a single component nematogen, 4-*n*-pentyl-4'-cyanobiphenyl (abbreviated 5CB)<sup>30</sup> and a four-component mixture of biphenyls and a terphenyl, E7.<sup>30</sup> 5CB and E7 have been used in some of our previous PDLC studies.<sup>5,9,12</sup> The crystal-nematic (KN) transition temperature,  $T_{\text{KN}}$ , of 5CB is  $\sim 298$  K; its nematic-isotropic (NI) transition occurs at  $T_{\text{NI}} \approx 309$  K, with enthalpy  $\Delta H_{\text{NI}}(5\text{CB}) = 0.85$  cal/g. If rapidly cooled from the nematic, 5CB can form a glassy state which crystallizes upon rewarming.<sup>12</sup> E7 easily forms a glassy nematic upon cooling, and crystallization does not readily occur upon rewarming. Instead the glass gradually becomes a fluid nematic. The NI transition of E7 occurs at  $T_{\text{NI}} \approx 330$  K<sup>5</sup> with  $\Delta H_{\text{NI}}(\text{E7}) = 1.09$  cal/g. The densities of 5CB and E7 are comparable (1.028 and 1.023 g/cm<sup>3</sup>, respectively).

**Matrix.** The matrix material chosen was Norland ultraviolet-curable optical adhesive 65 (abbreviated NOA65).<sup>31</sup> This mixture of monomers, oligomers, and a photoinitiator has also been used in several of our previous studies.<sup>2,7,8,9</sup> In the present work, NOA65 was the matrix in studies both of uncured LC/matrix mixtures and of mixtures with various degrees of cure. Its density (1.12 g/cm<sup>3</sup>) is slightly greater than those of the LCs.

**Mixture Preparation.** Mixtures of liquid crystal and uncured NOA65 were prepared using previously described techniques.<sup>7,8</sup> Small quantities (typically enough to produce a total volume of 100  $\mu\text{l}$ ) of NOA65 and LC were measured into a watch glass using precision micropipettes. The components were then vigorously stirred until a uniform mixture was obtained (generally 30 to 60 s was sufficient time). For studies of E7/NOA65 mixtures in the uncured state, about 10  $\mu\text{l}$  of sample were pipetted into an aluminum sample pan which was hermetically sealed by means of a cold welding tool.<sup>5,32</sup> For mixtures which were to be cured, about 5  $\mu\text{l}$  of sample were transferred to a custom-made gold-plated copper DSC pan



and then covered with an ultrathin (0.1–0.2 mm) quartz disc.<sup>8</sup> The disc rested on a shoulder around the pan bottom so as to give a sample of uniform thickness (on the order of 100 to 200  $\mu\text{m}$ ). Thickness uniformity was necessary to produce uniform cure rates throughout the sample upon exposure to UV radiation. The pan's gold coating insured that the sample would not react with the container material.

### Measurement Techniques

**Calorimetry.** The differential scanning calorimeter used in these studies was a Perkin-Elmer DSC2 instrument.<sup>32</sup> Operated isothermally, it permits determination of the rate of heat evolution,  $dQ/dt$ , during cure and of its integral,  $\Delta Q$ , the heat released during part or all of the cure process. Since both calorimeter and calorimetric methods have been previously described,<sup>5,6,8</sup> we shall only briefly review the essential features of the techniques at this time.

**Isothermal calorimetry.** The DSC system has been modified to allow introduction of ultraviolet radiation into the sample chamber so that kinetics and energetics of a UV-induced cure process can be determined from plots of  $dQ/dt$  versus  $t$ . The UV irradiation was provided by a 100 watt high pressure mercury lamp mounted in an ITI Model 15060 UV source<sup>33</sup> and was introduced into the calorimeter by an ultraviolet light guide.

A typical heat release curve for complete UV-cure of a PDLC is shown in Figure 1, where the exothermic power associated with the cure process is plotted versus time. The baseline is flat during the initial period when no UV irradiation occurs. As soon as sample irradiation begins, an abrupt increase in exothermic power occurs, followed by an almost exponential decay. The offset in baseline at the end of the trace with respect to that at the beginning is due to a difference in absorbance of UV by the sample and reference pans of the calorimeter and is of no consequence for the determination of kinetics or energetics of the cure process provided the final (UV on) baseline is used for analysis. The total heat release during cure,  $\Delta Q_{\text{cure}}$ , for such curves can be determined by integration using standard calorimeter software.<sup>32</sup>  $\Delta Q_{\text{cure}}$  is of particular importance for studies of PDLCs since it is a direct measure of degree of cure.<sup>34</sup>

For some LC/matrix mixtures the effects of  $D_{\text{cure}}$  were studied by an incremental

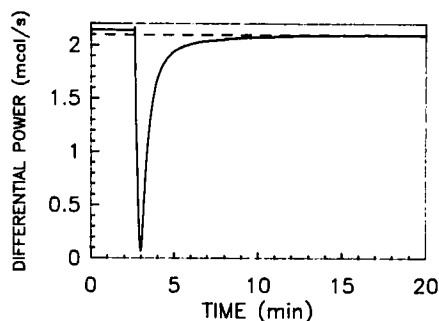


FIGURE 1 Plot of  $dQ/dt$  versus time for UV cure of a liquid crystal/NOA65 mixture. Such curves make it possible to determine  $\Delta Q_{\text{cure}}$ , the total heat released during cure, and  $\tau_{\text{cure}}$ , the time constant for the cure process. By convention, exotherms are taken as downward-going.

cure procedure. In this technique a sample was exposed to UV for times as short as 20–30 s to achieve a partial cure. Phase behavior of the sample in states of increasing cure was determined by scanning calorimetry (see next section) prior to the initial UV exposure and following each subsequent incremental cure step. This sequence of cure steps was continued until final cure was as complete as possible. Measurement of the heat release,  $\Delta Q$ , for each step made it possible to calculate the cumulative degree of cure (in percent) by summing the  $\Delta Q$  values:

$$D_{\text{cure}} = 100 \left( \sum \Delta Q \right) / \Delta Q_{\text{cure}}, \quad (14)$$

where the sum is over all incremental cure steps prior to a given DSC phase behavior determination, and  $\Delta Q_{\text{cure}}$  is the total heat release for all the cure steps.

**Scanning calorimetry.** The differential scanning calorimetry technique for determining PDLC phase behavior has also been described previously.<sup>5,6,8</sup> For these studies the calorimeter was operated in its temperature scanning mode: after a sample had been cooled to  $\sim 200$  K, its temperature was programmed linearly (at 20 K/min) over the range of interest while changes in the sample's heat absorption rate were recorded. Temperatures and specific heat increases of glass transitions were determined using software provided by the manufacturer.<sup>32</sup> The same software could likewise be used to analyze specific heat decreases associated with mixing. A standard program was also available to determine temperatures and enthalpies of first order phase transitions (e.g., melting and nematic-isotropic transitions).

Figure 2 shows DSC temperature scans for the two liquid crystals used in this study. The thermal spectrum of 5CB exhibits six features. The baseline shift at about 210 K is the LC glass transition. The other thermal events (from low to high temperature) are: a crystallization exotherm; a small endotherm (perhaps a crystal-crystal transition); a second exotherm; a large endothermic peak at the crystal-nematic (KN) transition temperature,  $T_{\text{KN}}$ ; and a small NI transition endotherm. The thermal spectrum of E7 shows only two features: the glass transition and the nematic-isotropic peak. DSC methods for obtaining values of the specific heat increment,  $\Delta C_g$ , at the glass transitions and magnitudes of the NI transition enthalpy,  $\Delta H_{\text{NI}}$ , have been previously described.<sup>5,6,8</sup>

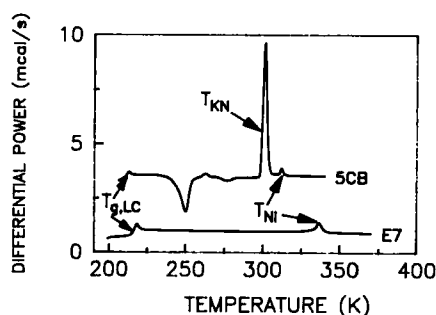


FIGURE 2 DSC thermal spectra for the two liquid crystals used in the present studies. The specific transitions are discussed in the text. Endotherms are upward-going.

In Figure 3 are shown thermal spectra for uncured and cured NOA65. That for the uncured sample exhibits a glass transition at about 210 K (close to  $T_g$  for the liquid crystals). Following cure at 300 K, the glass transition has shifted to 273 K due to the greatly reduced mobility of the large polymer molecules compared to that of the monomers and oligomers of the initial mixture. The magnitude of the specific heat change is essentially the same both before and after cure ( $\Delta C_g \sim 0.103$  cal/g-K).

In the Results section we shall examine thermal spectra for LC/matrix mixtures in various states of cure.

**Specific heat measurement.** As mentioned above, we used DSC to measure the specific heat both of the uncured mixtures and of their components (E7 and NOA65) in order to determine (from Equation 1) whether the apparent decrease in specific heat at the mixing temperature is, indeed, due to  $\Delta C_{\text{mix}} < 0$ . Measurements were carried out in a manner similar to that described in Reference 18 using scan rates of 20 K/min. Standard software<sup>32</sup> was employed for the analysis. Specific heat curves for pure E7 and uncured NOA65 are given in Figure 4. The peak in the curve for E7 is, of course, due to the NI transition; true values of the specific heat were thus not obtainable in the vicinity of this peak ( $T > 300$  K).

## EXPERIMENTAL RESULTS AND ANALYSIS

### Uncured E7/NOA65 Mixtures

**Thermal Spectra.** Thermal spectra for uncured E7/NOA65 mixtures with 14 different LC volume percentages,  $X$  ( $=100x$ ), are shown in Figure 5. All the samples show a specific heat increase at about 215 K. This transition is presumably due to the superposition of the glass transitions of the liquid crystal and the uncured NOA65, both of which occur at about the same temperature.

Although the samples with  $X = 0\%$  and  $10\%$  show no further transitions, those with concentrations in the range  $27.5\% - 80\%$  exhibit negative baseline shifts (that for  $X = 50\%$  is indicated by " $T_{\text{mix}}$ " in the figure). These shifts occur at the mixing temperature and are assumed to be due, at least in part, to decreases in the specific heat of mixing of the components ( $\Delta C_{\text{mix}} < 0$ ). The magnitudes and temperatures

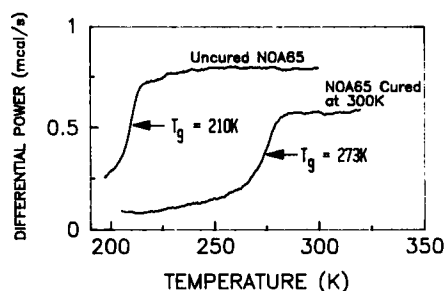


FIGURE 3 DSC thermal spectra for uncured and cured NOA65, the matrix material used in the present study.

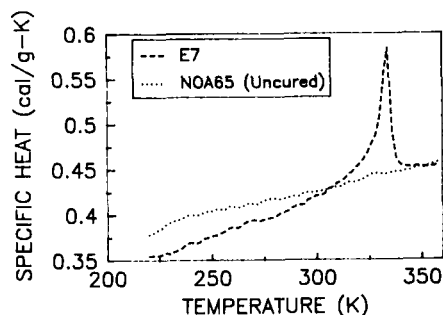


FIGURE 4 Specific heats of liquid crystal E7 and uncured NOA65 for use in Equation 1.

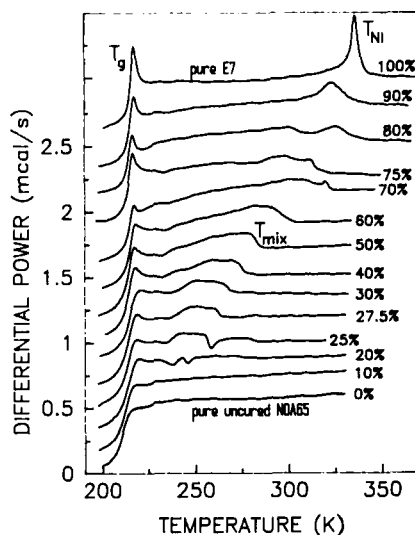


FIGURE 5 DSC thermal spectra for a series of uncured E7/NOA65 mixtures. The various transitions are discussed in the text.

of  $\Delta C_{\text{mix}}$  were determined using the DSC glass transition analysis software.<sup>32</sup> The more complicated behavior of samples with  $X = 20\%$  and  $25\%$  is discussed in the next paragraph. Mixtures with  $X = 70\%$ – $100\%$  exhibit a high temperature peak, the nematic-isotropic transition, the amplitude of which increases with  $X$ . For  $X \geq 90\%$  no mixing transition is observed; only the NI peak is seen.

We suspected that the complicated behavior for  $X = 20\%$  and  $25\%$  might be due to kinetic effects associated with the low temperature glass transition. In order to minimize these possible effects, we allowed samples with each of the two concentrations to soak at  $225\text{ K}$  (above  $T_g$ ) for several hours before a temperature scan was initiated. In Figure 6 the resulting scans are compared with the full range spectra. Although not conclusive, the “soak” scans do give a more positive indication of specific heat transitions. As will be seen below, these concentrations are close to the solubility limits of E7 in the matrix-rich phase, so that any thermal effect due to mixing would be expected to be small. At any rate, the results for  $X$

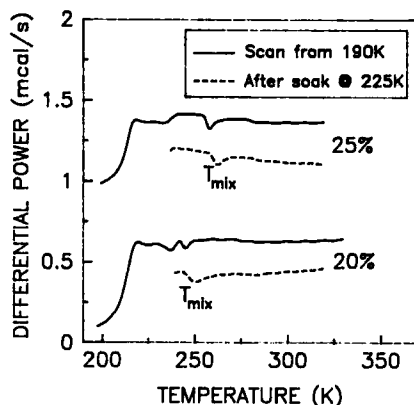


FIGURE 6 DSC thermal spectra for uncured E7/NOA65 mixtures containing 20% and 25% LC, with and without soak treatment discussed in the text.

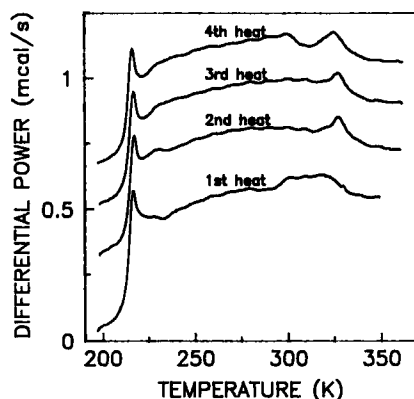


FIGURE 7 DSC thermal spectra for uncured E7/NOA65 mixture (LC concentration = 80% by volume) taken on successive temperature scans.

= 20% and 25% are not essential for constructing a phase diagram for the uncured E7/NOA65 system.

The sample for  $X = 80\%$  likewise showed complicated behavior, probably as a result of the proximity of this concentration to the upper solubility limit (of NOA65 in the LC-rich phase). As seen in Figure 7, sequential thermal spectra, each taken after cooling to  $\sim 190$  K, are different from one another. We ascribe these differences to variances in degree of mixing. We presume that the fourth scan is that for the most completely mixed system and is thus most nearly characteristic of the equilibrium state.

**Phase Diagram.** In Figure 8 is shown the UCST phase diagram derived from thermal scans like those of Figures 5–7. The plot is qualitatively similar to the theoretical curve of Reference 10 for an uncured mixture. The maximum temperature,  $T_c$  ( $\approx 307$  K), is just perceptible near  $X = 75\%$ . (Thus, for best PDLC formation, the cure temperature must be suitably higher than 307 K.) Although the scatter in the nematic-isotropic transition temperature is appreciable, the ex-

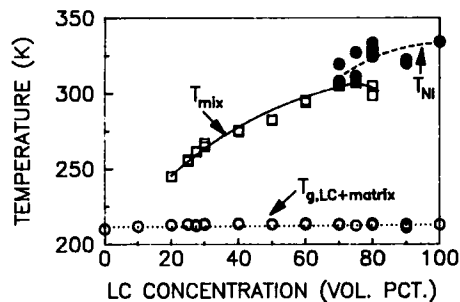
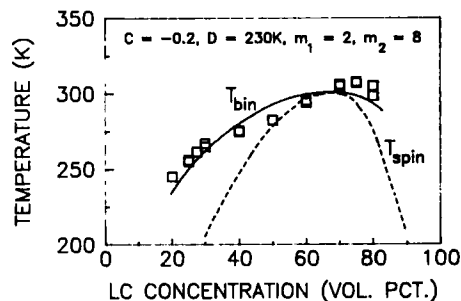


FIGURE 8 Phase diagram for uncured E7/NOA65 mixtures.

FIGURE 9 Measured and calculated mixing temperatures for uncured E7/NOA65 system. Points are  $T_{\text{mix}}$  values from Figure 8. Solid line is Flory-Huggins binodal curve; dashed line is corresponding spinodal curve.

istence of the nematic phase for  $X \geq 70\%$  seems to be clearly established. As already seen in Figure 5, the glass transition temperature is independent of concentration. In Figure 9 are plotted spinodal<sup>11</sup> and binodal curves<sup>35</sup> calculated from the F-H theory for  $C = -0.2$ ,  $D = 230$  K,  $m_1 = 2$ , and  $m_2 = 8$ . Agreement of the equilibrium binodal curve with experiment is reasonable. Here  $m_1$  is taken to be the degree of polymerization for the liquid crystal,  $m_2$  that for the uncured matrix. Thus, for best agreement, we must assume that the weight of an average matrix molecule is about four times that of an average LC molecule. (In fact, the average molecular weight of uncured NOA65 is  $\sim 415$ <sup>36</sup> and that of E7  $\sim 272$ .)

**$\Delta C_{\text{mix}}$  from Thermal Spectra.** Equation 13 predicts that  $\Delta C_{\text{mix}}$  should show a minimum at a concentration  $X = 50\%$ . Experimental values of  $\Delta C_{\text{mix}}$ , derived from thermal spectra like those of Figure 5, are plotted in Figure 10 and show the expected minimum, shifted to slightly higher concentrations. Indeed, a better fit to the data than that of Equation 13 is given by

$$\Delta C_{\text{mix}} = \text{const}(x - 0.15)(0.95 - x), \quad (15)$$

a relation which indicates that the solubility of E7 in the NOA65-rich phase is  $\sim 15\%$  while that of NOA65 in the E7-rich phase is  $\sim 5\%$ .

**$\Delta C_{\text{mix}}$  from Specific Heat Measurements.** Specific heat measurements confirm the presumption that the apparent decreases in specific heat at  $T_{\text{mix}}$  (Figures 5–7)

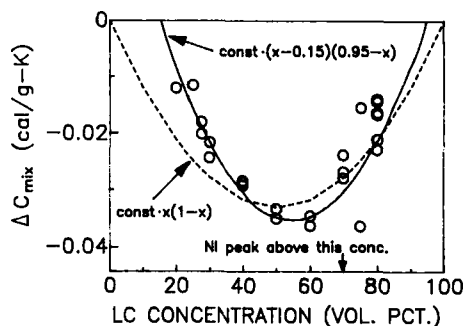


FIGURE 10 Excess specific heat of mixing for uncured E7/NOA65 mixtures.  $\Delta C_{\text{mix}}$  values were determined from DSC scans like those of Figure 5. Curves are discussed in the text.

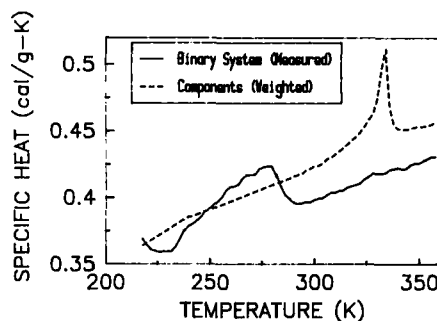


FIGURE 11 Specific heat of uncured [1:1] E7/NOA65 mixture (solid curve) compared to weighted value for individual components. It is clear that  $\Delta C_{\text{mix}}$  is negative for temperatures greater than 284 K, the mixing temperature.

are due, at least in part, to  $\Delta C_{\text{mix}} < 0$ . For  $\Delta C_{\text{mix}}$  to be negative, Equation 1a shows that  $C_b$  for the single-phase mixture should be less than the weighted sum for the components:  $zC_1 + (1 - z)C_2$ .<sup>37</sup> As seen in Figure 11, for  $T > 284$  K, the specific heat of the 50% binary mixture is, indeed, considerably lower than the weighted sum for the components. However, the magnitude of the greatest decrease ( $\sim -0.024$  cal/g-K) is somewhat smaller than that determined from Figure 10 ( $\sim -0.035$  cal/g-K). This discrepancy may be due to a positive contribution from the enthalpy of mixing to the experimental curve below  $T_{\text{mix}}$ . In Figure 11 we see that, for temperatures below  $T_{\text{mix}}$  (i.e., from  $\sim 246$  K to  $\sim 284$  K), the apparent specific heat of the mixture exceeds the weighted value of the components. The enthalpy associated with this excess is roughly 0.8 cal/g, a reasonable value for  $\Delta H_{\text{mix}}$  (see previous discussion of the F-H model). Specific heat plots for  $X = 30\%$  to  $60\%$ , like that of Figure 11, yield smaller values of  $\Delta C_{\text{mix}}$  than do the corresponding plots of Figure 5. For  $X = 20\%$  the specific heats of the mixture and of the weighted components are essentially equal. For  $X > 60\%$  the presence of the LC nematic-isotropic peak makes it impossible to make a comparison.

**Comparison with Gel Results of Hikmet *et al.*** It is useful to compare the minimum value of  $\Delta C_{\text{mix}}$  from Figure 10 ( $\sim -0.035$  cal/g) to that for the high temperature specific heat decrease of the cyclohexanol/polystyrene gel of Hikmet *et al.*<sup>24</sup> Although they did not state the magnitudes of their two specific heat steps, we can

estimate them. The increase in specific heat at low-temperature is due to the glass transition of the gel; typically  $\Delta C_g$  values for such transitions are on the order of  $+0.1$  cal/g-K. Since, for gels of 29% and 50% polymer content, the step at the mixing temperature is negative and roughly half the magnitude of  $\Delta C_g$ , we obtain  $\Delta C \sim -0.05$  cal/g-K for mixing in the gel. The fact that this value is comparable to that for our minimum  $\Delta C_{\text{mix}}$  suggests that the high temperature specific heat step of Hikmet *et al.* is, indeed, due to the (negative) excess specific heat of mixing of this UCST system.

**Nematic-isotropic Transition.** It is known<sup>5,6,8,12</sup> that  $\Delta H_{\text{NI}}$ , the nematic-isotropic transition enthalpy of a LC/matrix system, is proportional to  $\alpha$ , the fraction of liquid crystal which is phase-separated from the polymer matrix, with  $\alpha$  given by:

$$\alpha = (1 + \rho_p V_p / \rho_{\text{LC}} V_{\text{LC}}) \Delta H_{\text{NI}} / \Delta H_{\text{NI}}(\text{LC}). \quad (16)$$

Here  $\rho_p$  and  $\rho_{\text{LC}}$  are the polymer and LC densities, and  $V_p$  and  $V_{\text{LC}}$  are their volumes in the mixture. Figure 12 plots  $\Delta H_{\text{NI}}$  versus LC concentration for uncured E7/NOA65 mixtures. The appreciable scatter for  $X = 80\%$  reflects the previously mentioned difficulties in obtaining uniform mixing. The plot makes it clear that no phase-separation to form a nematic phase occurs for LC concentrations below about 70%, as already suggested by Figure 8. From Equation 16 we find that the amount of liquid crystal which has separated from the matrix is no more than 4% for a LC concentration of 70%, increasing to  $\sim 14\%$  for  $X = 80\%$  and to  $\sim 67\%$  for  $X = 90\%$ .

### Effect of Degree of Cure

**E7/NOA65 System.** As mentioned above, the influence of  $D_{\text{cure}}$  on phase separation was studied using an incremental cure procedure. In Figure 13 are shown plots of  $dQ/dt$  versus  $t$  for a sequence of five isothermal UV-cure steps of a 50% E7/NOA65 mixture. The cure temperature was 300 K. DSC thermal spectra were recorded prior to the initial cure step and following each subsequent incremental cure. Thus, phase behavior was determined for a sample in six different degrees of cure:  $D_{\text{cure}} = 0\%, 48.4\%, 68.9\%, 76.1\%, 83.0\%$ , and  $100\%$ .

The DSC thermal spectra for the six degrees of cure are shown in Figure 14.

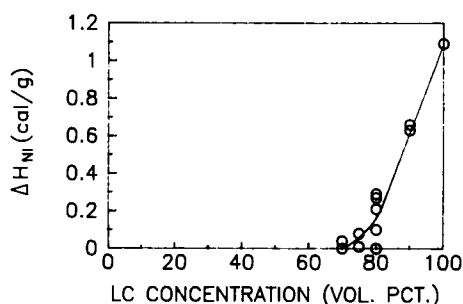


FIGURE 12 Nematic-isotropic transition enthalpy for uncured E7/NOA65 mixtures. Clearly, the nematic phase does not exist for LC concentrations below 70%.



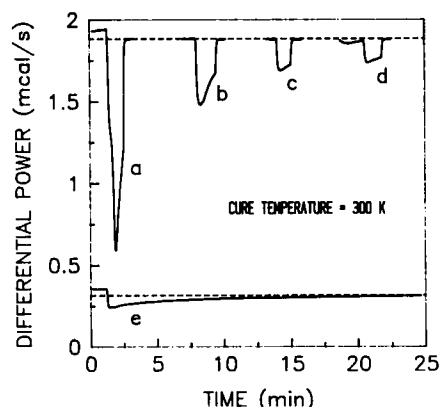


FIGURE 13 Isothermal heat release curves for sequential cure steps of a [1:1] E7/NOA65 mixture. The values of  $\Delta Q$  for the successive steps are: a) 14.2, b) 5.9, c) 2.2, d) 2.0, and e) 5.0 cal/g. The corresponding degrees of cure (from Equation 14) after each step are: a) 48.4%, b) 68.9%, c) 76.1%, d) 83.0%, and e) 100%.

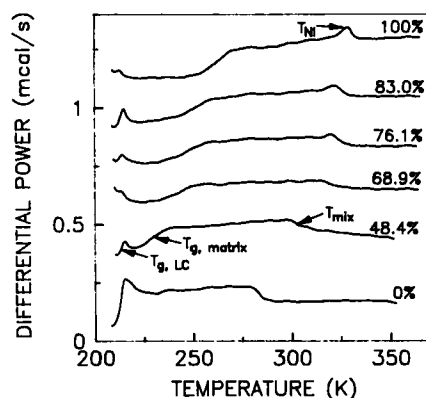


FIGURE 14 DSC thermal spectra for [1:1] mixtures of E7 and NOA65 with various degrees of cure.

Only two transitions are evident for  $D_{\text{cure}} = 0\%$ : a glass transition at  $\sim 215$  K (due to the superposition of the transitions of both LC and uncured matrix) and the mixing transition at  $\sim 280$  K. With increasing degree of cure, the matrix glass transition moves to higher temperature, while that for the liquid crystal remains essentially fixed.

Of greater interest is the mixing transition. For  $D_{\text{cure}} = 0\%$ , 48.4%, and 68.9% the temperature of this transition increases while the magnitude of  $\Delta C_{\text{mix}}$  decreases. For  $D_{\text{cure}} = 76.1\%$  and 83.0% a nematic-isotropic peak is superimposed on the mixing transition. Thus, for these samples, the NI and mixing transitions occur almost simultaneously. This result seems reasonable: Sigaud *et al.*<sup>38</sup> have pointed out that, for solutions of liquid crystalline side-chain polymers in low molecular weight LCs, the polymer solubility is lower in the nematic phase than in the isotropic phase. Thus, in our case, it is not surprising that mixing should occur just above the NI transition. The fully cured sample ( $D_{\text{cure}} = 100\%$ ) exhibits a typical PDLC thermal spectrum<sup>5,6,8</sup>: a low temperature glass transition of the LC, a matrix glass

transition, and a nematic-isotropic transition peak. There is no evidence for a mixing transition (i.e., no negative baseline shift), which indicates that phase separation has become essentially irreversible.

Data from Figure 14 and from similar DSC scans for several other samples have been used to construct the diagram of temperature versus degree of cure ( $T$ - $D_{\text{cure}}$  plot) of Figure 15. The increase in  $T_{g,\text{matrix}}$  and constancy of  $T_{g,\text{LC}}$  are clearly apparent, as is the increase in  $T_{\text{mix}}$  to merge with  $T_{\text{NI}}$ .

In Figure 16 are plots of  $-\Delta C_{\text{mix}}$  (the apparent decrease in specific heat at the mixing temperature, determined from thermal scans) as a function of degree of cure. The linear decrease of  $\Delta C_{\text{mix}}$  does not pass through 0 at  $D_{\text{cure}} = 100\%$ ; it appears that mixing ceases somewhere in the range  $83\% < D_{\text{cure}} < 100\%$ . This conclusion is supported by Figure 17 where  $\Delta H_{\text{NI}}$  (proportional to the amount of phase-separated LC) is plotted versus degree of cure for  $X = 50\%$ . It is clear that the matrix must be more than 70% cured before phase separation commences. Equation 16 reveals that less than 10% of LC has phase separated for  $D_{\text{cure}} = 84\%$ . Apparently most of the demixing occurs during the final 10% of cure. For a fully cured sample, Equation 16 gives  $\alpha \approx 0.5$ , a value comparable to that for E7/NOA65 cured in one step and for a similar UV-cured system.<sup>8</sup> Thus, even when cure is complete (as in a E7/NOA65 PDLC) about half the LC remains dissolved in the matrix. (However, the LC solubility decreases upon cooling.<sup>12</sup>)

**5CB/NOA65 System.** Since E7 is a multicomponent LC, its solubility behavior

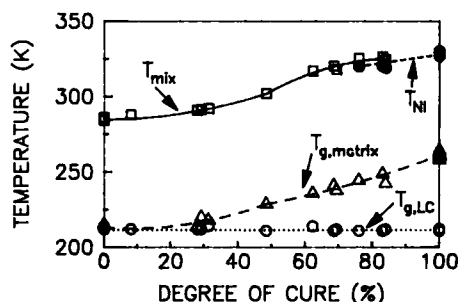


FIGURE 15 Dependence of transition temperatures on degree of cure for [1:1] mixtures of E7 and NOA65.

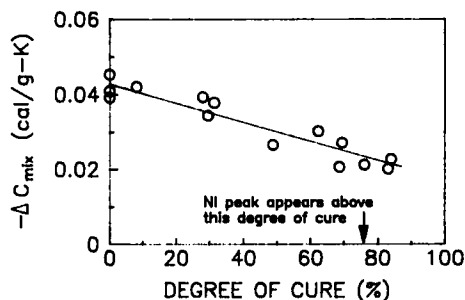


FIGURE 16 Dependence of (negative) excess specific heat of mixing on degree of cure for [1:1] mixtures of E7 and NOA65. Values of  $\Delta C_{\text{mix}}$  were determined from DSC thermal spectra like those of Figure 14.

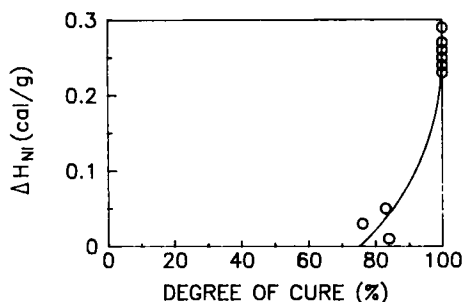


FIGURE 17 Dependence of nematic-isotropic transition enthalpy on degree of cure for [1:1] mixtures of E7 and NOA65.

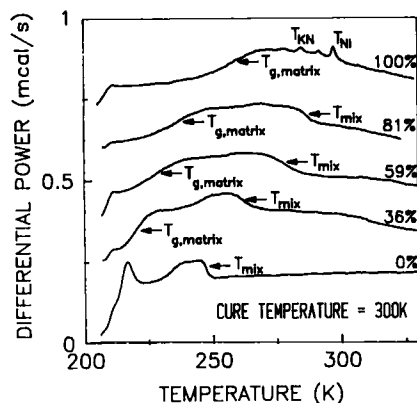


FIGURE 18 DSC thermal spectra for a [1:1] mixture of 5CB and NOA65 with various degrees of cure.

is complicated by the possibility that certain of its components may preferentially dissolve in the NOA65 matrix. Therefore, it seemed advisable to carry out experiments using a single component liquid crystal, 5CB.

The incremental cure procedure discussed above was used to obtain [1:1 (by volume)] mixtures of 5CB/NOA65 with 5 different values of  $D_{\text{cure}}$ ; the cure temperature was 300 K. Thermal spectra for those samples are plotted in Figure 18. As in the case of E7/NOA65, the matrix glass transition temperature and the mixing temperature both increase with increasing  $D_{\text{cure}}$ , while the LC glass transition temperature remains constant. The NI transition peak does not appear until after the final cure step; as a result of impurities, its temperature is  $\sim 297$  K, some 12 K lower than for the pure LC. Two weak peaks (at  $\sim 285$  K and 292 K) have also appeared during final cure. From their temperatures we conclude that the peak at 285 K is a transition involving a metastable crystal and that at 292 K is due to melting. Relative to the corresponding peaks of the pure LC (Figure 2), the melting peak for  $D_{\text{cure}} = 100\%$  is much more greatly reduced than is the NI peak. This reduction suggests that the confinement of LC in microdroplets which results from matrix cure<sup>1-4</sup> promotes glass formation rather than crystallization.

Figure 19 is a  $T$ - $D_{\text{cure}}$  diagram derived from the thermal spectra of Figure 18. The diagram is similar to that for E7/NOA65 (Figure 15).

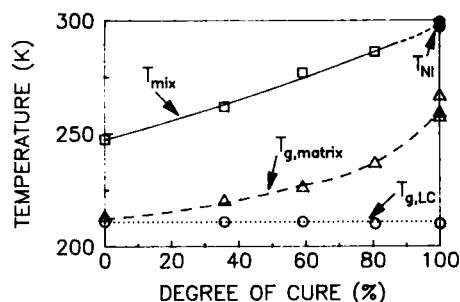


FIGURE 19 Dependence of transition temperatures on degree of cure for a [1:1] mixture of 5CB and NOA65.

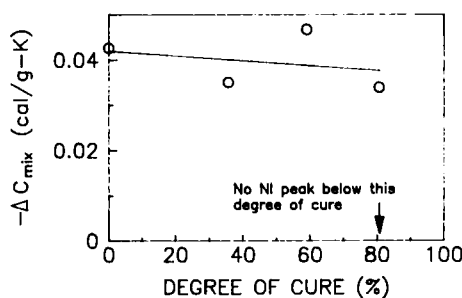


FIGURE 20 Dependence of (negative) excess specific heat of mixing on degree of cure for a [1:1] mixture of 5CB and NOA65.  $\Delta C_{\text{mix}}$  values were determined from DSC thermal spectra of Figure 18.

In Figure 20  $-\Delta C_{\text{mix}}$  (from the DSC thermal scans) is plotted versus degree of cure. Although the scatter is too great to accurately discern the dependence on  $D_{\text{cure}}$ , it is clear that the magnitude of  $\Delta C_{\text{mix}}$  is about equal to that for the E7/NOA65 mixtures (Figure 16). This result may be related to the fact that the molecular weights of the two LCs are comparable (272 for E7, 249 for 5CB).

Immediately after cure,  $\alpha$  values derived from  $\Delta H_{\text{NI}}$  vary considerably. The incremental cure process seems to lead to a lower degree of cure (i.e., a smaller value of  $\Delta Q_{\text{cure}}$ ) and hence to less phase separation ( $\alpha \sim$  a few percent) than does a one-step cure ( $\alpha$  values from 15% to 70%). Furthermore, both  $T_{\text{KN}}$  and  $T_{\text{NI}}$  are depressed  $\sim 10$  K. However, after an extended post-cure period ( $>1$  year), all samples have similar values of  $\alpha$  (12% to 17%), and the KN and NI transition temperatures are comparable to those of the pure LC. Evidently cure reactions continue long after the cessation of UV irradiation, leading to similar degrees of cure for all samples. In the process, matrix molecules apparently diffuse out of the liquid crystal, leaving it much more pure than it had been directly after cure.

## CONCLUSIONS

The major conclusions of this research address two aspects of phase separation in LC/polymer mixtures: the effect of LC concentration in uncured systems and the influence of the degree of cure.

*Phase Separation in Uncured Liquid Crystal/Matrix System.* Using differential scanning calorimetry, we have carried out the first direct determinations of the (negative) excess specific heat of mixing of a UCST binary system: uncured E7/NOA65 mixtures with various LC concentrations. A step-like baseline decrease was detected in DSC thermal spectra and assumed to be due primarily to  $\Delta C_{\text{mix}}$ . Measurements of the specific heats of both the mixtures and their components confirmed the correctness of this conclusion. Comparison of specific heat and DSC thermal spectra results suggest that a small endotherm due to  $\Delta H_{\text{mix}}$ , the excess heat of mixing, may also contribute to the mixing transition. The magnitudes of  $\Delta C_{\text{mix}}$  for the uncured E7/NOA65 mixtures are comparable to experimental and theoretical values for binary polymer LCST systems.<sup>17,18</sup> A plot of  $\Delta C_{\text{mix}}$  versus LC concentration exhibits a minimum, as expected from theory. From the plot we can estimate the solubility limit of E7 in the NOA65-rich phase ( $\sim 15\%$ ) and of NOA65 in the E7-rich phase ( $\sim 5\%$ ).

The phase diagram for the uncured E7/NOA65 system calculated using the Flory-Huggins model agrees fairly well with experiment. The F-H model also predicts the correct sign for  $\Delta C_{\text{mix}}$ , but is less successful in calculating its magnitude.

DSC thermal spectra of samples with high values of  $X$ , the liquid crystal concentration, reveal the presence of a NI transition peak. From the enthalpy of that transition we can estimate the amount of LC which has phase-separated from the matrix. No more than 4% of the LC crystal has demixed for  $X = 70\%$ , increasing to  $\sim 14\%$  for  $X = 80\%$  and to  $\sim 67\%$  for  $X = 90\%$ .

The maximum mixing temperature of the uncured E7/NOA65 mixtures is slightly above 300 K. To avoid undesired phase separation prior to final cure, the formation temperature for an E7/NOA65 polymer-dispersed liquid crystal (PDLC) should thus be suitably higher than 300 K.

*Effect of Degree of Cure on Phase Separation.* Phase separation in E7/NOA65 and 5CB/NOA65 mixtures was studied as a function of degree of cure, which was varied by a step-wise incremental UV-cure of the polymer matrix. Both mixing and phase transitions were determined from successive DSC thermal spectra. The mixing transition merged smoothly with the nematic-isotropic transition, in accord with the observation<sup>38</sup> that a polymer dissolves better in the isotropic phase than in the nematic. The magnitudes of  $-\Delta C_{\text{mix}}$  for partially cured E7/NOA65 and 5CB/NOA65 mixtures are comparable ( $\sim 10^{-2}$  cal/g-K).

Separation of the liquid crystal phase from the matrix seems to take place when the cure process nears completion. Only during the last 10%, or so, of cure does phase separation of the LC from the matrix become "frozen in." Once this has occurred, mixing can no longer take place, although some liquid crystal remains permanently dissolved in the matrix. The appearance of a nematic-isotropic peak during the final cure stages confirms that phase separation has become more-or-less permanent. Furthermore, the magnitude of the NI transition enthalpy makes it possible to estimate the amount of LC which has phase-separated from the matrix.<sup>5,6,8,12</sup> For an E7/NOA65 system, the value of  $\alpha$  rises from less than 10% to 50% as the degree of cure increases from 84% to 100%.

Cure of NOA65 to form a PDLC using 5CB, a liquid crystal which readily

crystallizes when pure, tends to suppress crystallization. Evidently, confinement of the LC to microdroplets favors the glassy state.

## APPENDIX: CONSTRAINTS ON F-H PARAMETERS\*

As discussed above, Nishi<sup>14</sup> has shown that for a UCST system,  $C < 0$  and  $D > 0$ , while for a LCST blend  $C > 0$  and  $D < 0$ . However, additional constraints on  $C$  and  $D$ , as well as on  $m_1$  and  $m_2$ , can also be derived using Equation 7 and the schematic phase diagrams in Figure A1.

*UCST System.* As is evident from Figure A1a,

$$T \leq T_c \text{ or } 1/T \geq 1/T_c. \quad (\text{A1})$$

Thus, from Equation 7,

$$1/T \geq -C/D + \epsilon', \quad (\text{A2})$$

where

$$\epsilon' = (2D)^{-1}[m_1^{-0.5} + m_2^{-0.5}]^2 \quad (\text{A3})$$

Since  $D > 0$  for a UCST system,  $\epsilon'$  is positive definite and we can write

$$-C/D < 1/T \quad (\text{A4})$$

which becomes (again using  $D > 0$ ):

$$C > -D/T. \quad (\text{A5})$$

Therefore, for a UCST system  $C$  lies above the line  $C = -D/T$ .

*LCST System.* We must be careful in our handling of inequalities with this case because  $D < 0$ . From Figure A1b we have

$$T \geq T_c \text{ or } 1/T \leq 1/T_c. \quad (\text{A6})$$

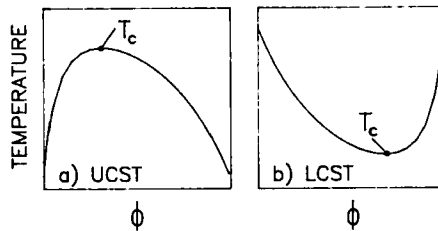


FIGURE A1 Schematic UCST and LCST phase diagrams.

\*Contains important contributions by G. Paul Montgomery, Jr.

From Equation 7:

$$1/T \leq -C/D - \epsilon', \quad (\text{A7})$$

where  $\epsilon'$  is again positive definite and its minus sign results from the fact that  $D < 0$ . Using the fact that  $D = -|D|$ , we rewrite Equation A7 as

$$C/|D| \geq 1/T + \epsilon' \quad (\text{A8})$$

and

$$C \geq |D|/T + \epsilon', \quad (\text{A9})$$

or

$$C \geq -D/T + \epsilon'. \quad (\text{A10})$$

So that

$$C > -D/T. \quad (\text{A11})$$

Thus, for the LCST system, as well,  $C$  lies above the line  $C = -D/T$ .

Equation 7 also places constraints on the values that  $m_1$  and  $m_2$  can assume for an LCST system. Since  $T_c$  must be greater than zero, we require that

$$|1/2D| [m_1^{-0.5} + m_2^{-0.5}]^2 < |C/D| \quad (\text{A12})$$

or

$$[m_1^{-0.5} + m_2^{-0.5}]^2 < 2C. \quad (\text{A13})$$

Consequently, in order to have physically meaningful LCST phase diagrams,  $m_1$  and  $m_2$  must be sufficiently large. For a typical value of  $C$  (say,  $0.5^{15}$ ), equation A13 says that if  $m_1 = 2$ ,  $m_2$  must be at least 12. Actually,  $m_1$  and  $m_2$  should be somewhat larger than these values for temperatures which are reasonable in magnitude. Equation 7 places no such constraints on  $m_1$  and  $m_2$  for UCST systems since  $D > 0$ .

### Acknowledgment

I thank G. Paul Montgomery, Jr. for performing the calculation of the binodal curve of Figure 9 and for valuable contributions to the discussion of the inequalities governing the "C" and "D" parameters of the F-H model (see Appendix). I am grateful to Daniel B. Hayden for developing computer programs to extract thermal spectra from the calorimeter for use in preparing figures. I also thank Thomas H. VanSteenkiste (for assistance with DSC setup) and Nuno A. Vaz, T. S. Ellis, and R. J. Eldred (for discussions).

## References

A brief report of this work appeared in *Phys. Rev. Lett.* **70**, 198 (1993).

1. J. W. Doane, N. A. Vaz, B.-G. Wu and S. Zumer, *Appl. Phys. Lett.*, **48**, 269 (1986).
2. N. A. Vaz, G. W. Smith and G. P. Montgomery, Jr., *Mol. Cryst. Liq. Cryst.*, **146**, 1 (1987).
3. N. A. Vaz, G. W. Smith and G. P. Montgomery, Jr., *Mol. Cryst. Liq. Cryst.*, **146**, 17 (1987).
4. J. L. West, *Mol. Cryst. Liq. Cryst.*, **157**, 427 (1988).
5. G. W. Smith and N. A. Vaz, *Liq. Cryst.*, **3**, 543 (1988).
6. G. W. Smith, *Mol. Cryst. Liq. Cryst.*, **180B**, 201 (1990).
7. G. P. Montgomery, Jr., N. A. Vaz and G. W. Smith, *Proc. SPIE* **958**, 104 (1988).
8. G. W. Smith, *Mol. Cryst. Liq. Cryst.*, **196**, 89 (1991).
9. N. A. Vaz, G. W. Smith and G. P. Montgomery, Jr., *Proc. SPIE* **1257**, 9 (1990); *Mol. Cryst. Liq. Cryst.*, **197**, 83 (1991).
10. Y. Hirai, S. Niiyama, H. Kubai and T. Gunjima, *SPIE* **1257**, 2 (1990); *Reps. Res. Lab. Asahi Glass Co.*, **40**, 285 (1990). (The second, and longer, paper omits the references, which may be the same as those in the first.)
11. G. W. Smith, *Mol. Cryst. Liq. Cryst.*, **225**, 113 (1992). Equation 4 in this paper contains an error. It should read  $P(x) = \Delta C_{LC}(x)/\Delta C_{LC}(LC)$ .
12. G. W. Smith, G. M. Ventouris and J. L. West, *Mol. Cryst. Liq. Cryst.*, **213**, 11 (1992).
13. P. J. Flory, *J. Chem. Phys.*, **10**, 51 (1942). M. L. Huggins, *Ann. NY Acad. Sci.*, **43**, 1 (1942).
14. T. Nishi, *Rep. Prog. Polym. Phys. Jap.*, **20**, 225 (1977); *J. Macromol. Sci.-Phys.*, **B17**, 517 (1980); *CRC Crit. Revs. in Sol. State and Mater. Sci.*, **12**, 319 (1985). The UCST and LCST regions in Figure 1 of the first paper (Figure 3 of the second paper) appear to be incorrect. The UCST region in the 4th quadrant and the LCST region in the 2nd quadrant should both lie above the line  $C = -D/T$  (Nishi's notation:  $A = -B/RT$ ), not below it (see our Appendix). LCST parameters from Figure 5 of Nishi's first paper agree with this conclusion.
15. I. Sanchez, *Ann. Rev. Mater. Sci.*, **13**, 387 (1983).
16. J. Y. Kim and P. Palfy-Muhoray, *Mol. Cryst. Liq. Cryst.*, **203**, 93 (1991).
17. G. ten Brinke and F. E. Karasz, *Macromolecules*, **17**, 815 (1984).
18. R. S. Barnum, S. H. Goh, J. W. Barlow and D. R. Paul, *J. Polym. Sci.: Polym. Lett.*, **23**, 395 (1985).
19. A. Natansohn, *J. Polym. Sci.: Polym. Lett.*, **23**, 305 (1985).
20. M. Ebert, R. W. Garbella and J. H. Wendorff, *Makromol. Chem., Rapid Commun.*, **7**, 65 (1986).
21. C. Uriarte, J. I. Eguiazabal, M. Llanos, J. I. Iribarren and J. J. Iruin, *Macromolecules* **20**, 3038 (1987).
22. J. A. Moore and J.-H. Kim, *Macromolecules* **25**, 1427 (1992).
23. D. J. Walsh and S. Rostami, *Adv. Polym. Sci.*, **70**, 119 (1985).
24. R. M. Hikmet, S. Callister and A. Keller, *Polymer*, **29**, 1378 (1988).
25. W. Ahn, C. Y. Kim, H. Kim and S. C. Kim, *Macromolecules*, **25**, 5002 (1992).
26. A. F. M. Barton, *Handbook of Solubility Parameters and Other Cohesion Parameters*, CRC Press, Boca Raton, FL (1983), p. 263ff; A. F. M. Barton, *CRC Handbook of Polymer-Liquid Interaction Parameters and Solubility Parameters*, CRC Press, Boca Raton, FL (1990), p. 3ff.
27. A. Cumming, P. Wiltzius, F. S. Bates and J. H. Rosedale, *Phys. Rev. A*, **45**, 885 (1992).
28. In our systems volume fraction  $\approx$  mass fraction since component densities are comparable. Thus  $x$  represents both LC mass and volume fraction.
29. F. E. Karasz, private communication.
30. Manufactured by Merck Ltd, Poole, England. Distributed by EM Industries, Inc., Hawthorne, NY.
31. Norland Products, Inc., North Brunswick, NJ.
32. Perkin-Elmer Corp., Norwalk, CT.
33. Instrument Technology, Inc., Westfield, MA.
34. C. E. Hoyle, R. D. Hensel and M. B. Grubb, *J. Polymer Sci.*, **22**, 1865 (1984).
35. G. P. Montgomery, Jr. (private communication).
36. N. A. Vaz (private communication).
37. It should be noted that, since the densities of E7 and NOA65 are comparable (1.028 vs. 1.12 g/cm<sup>3</sup>), equation 1a yields almost identical results using either mass or volumetric LC concentrations.
38. G. Sigaud, M. F. Achard, F. Hardouin, C. Coulon, H. Richard and M. Mauzac, *Macromolecules*, **23**, 5020 (1990).